JSTT JOURNAL OF SCIENCE AND TRANSPORT TECHNOLOGY

Journal of Science and Transport Technology
Journal homepage: https://jstt.vn/index.php/en

UNIVERSITY OF TRANSPORT TECHNOLOGY

Impact of geological map scale on the performance of landslide susceptibility zonation using artificial intelligence models

Nguyen Duc Manh[1], Indra Prakash[2], Xuan-Kien Dang[3], Tran Xuan Bien[4], Nguyen Duc Dam[5,*]

[1]University of Transport and Communications, Cau Giay Street, Lang Ward, Hanoi, Vietnam

[2]DDG (R) Geological Survey of India, Gandhinagar 382010, India; indra52prakash@gmail.com (I.P.)

[3]University of Transport Ho Chi Minh City, 2, Vo Oanh, Thanh My Tay, Ho Chi Minh 700000, Vietnam; kien.dang@ut.edu.vn

[4]Hanoi University of Natural Resources and Environment No. 41A Phu Dien Street, Phu Dien Ward, Hanoi City, Vietnam; txbien@hunre.edu.vn

[5]Geotechnical Engineering and Artificial Intelligence research group, University of Transport Technology, 54 Trieu Khuc, Thanh Liet, Hanoi, Vietnam

Article info
Type of article:
Original research paper

DOI:
https://doi.org/10.58845/jstt.utt.2026.en.6.3.93-111

***Corresponding author:**
Email address:
damnd@utt.edu.vn

Received: 18/03/2026
Received in Revised Form: 26/05/2026
Accepted: 24/06/2026

Abstract: This study assesses the impact of geological map scale on the performance of artificial intelligence (AI) models in landslide susceptibility zonation (LSZ) along the Tuyen Quang–Ha Giang Highway, northern Vietnam. For this purpose, a total of 139 past landslide locations and 14 conditioning factors were collected and used for generating training (70%) and testing (30%) datasets. Four AI models: Artificial Neural Network (ANN), Convolutional Neural Network (CNN), Deep Neural Network (DNN) and a hybrid CNN–DNN model were developed and used for landslide modeling at two geological map scales: a small-scale map (1:200000) and a large-scale map (1:50000). Model accuracy was evaluated using AUC/ROC and multiple statistical indices. Results of this study showed that all models demonstrated effective predictive performance (AUC = 0.89–0.97), with the hybrid CNN–DNN model achieving the best performance and generalization. The models using the larger-scale geological map yielded higher spatial precision and better delineation of high and very high susceptibility zones compared to those used the smaller-scale geological map. The SHAP analysis revealed that maximum rainfall, average annual rainfall, vegetation cover (NDVI), elevation, and proximity to roads were the most influential factors to the predictive capability of the models. The study also highlights the importance of AI-based models, particularly deep learning and hybrid architectures in capturing complex nonlinear relationships among conditioning factors, improving prediction accuracy, and enhancing the reliability of LSZ for hazard management and infrastructure planning in mountainous regions.

Keywords: Landslide susceptibility, geological map scale, artificial intelligence, CNN–DNN, Vietnam.

1. Introduction

Landslides are among the most frequent and devastating geological hazards, causing extensive loss of life, damage to infrastructure, and economic disruption worldwide. They involve the downslope movement of soil, rock, or debris under gravity when the driving shear stress exceeds the resisting shear strength of slope materials. Globally, landslides result in annual economic losses exceeding USD 3 billion and claim thousands of lives [1]. The hazard is particularly acute in mountainous regions, where steep terrain, fractured bedrock, and intense monsoonal rainfall interact with anthropogenic disturbances such as road construction, deforestation, and unplanned urban expansion. Climate change has further intensified extreme precipitation events, increasing landslide frequency and magnitude, especially in developing countries where slope management and land-use control are inadequate.

Landslide Susceptibility Zonation (LSZ) aims to delineate areas vulnerable to slope failure by correlating past landslide occurrences with conditioning factors such as topography, lithology, hydrology, vegetation, and human activity. Traditional qualitative approaches rely heavily on expert judgment and subjective weighting of these factors, which may reduce reproducibility and introduce bias. Quantitative and statistical methods such as frequency ratio (FR) [2], logistic regression (LR) [3] or weight of evidence (WoE) [4] offer greater objectivity but often struggle to capture complex nonlinear relationships among variables that govern slope instability.

In recent years, artificial intelligence (AI) and machine learning (ML) models have transformed LSZ mapping by enabling data-driven prediction and nonlinear pattern recognition. Techniques such as Artificial Neural Networks (ANN) [5], Support Vector Machines (SVM) [6] and Random Forests (RF) [7] have achieved high accuracy in identifying landslide-prone zones [8, 9]. More recently, deep learning (DL) architectures such as the Convolutional Neural Network (CNN) [10] and Deep Neural Network (DNN) [11] have shown superior capability in feature extraction, hierarchical representation, and spatial pattern learning from high-dimensional geospatial datasets. Among these, hybrid models (e.g., CNN–DNN) integrate the strengths of both architectures, offering improved generalization and higher precision in complex terrain conditions. The use of such advanced AI approaches in LSZ not only enhances prediction accuracy but also provides interpretable and transferable models for regional-scale hazard management [12].

While the importance of AI-based models in LSZ has been widely recognized, the impact of geological map scale as a fundamental spatial variable on model performance remains insufficiently understood. The geological map scale determines the level of spatial detail, influencing how lithological boundaries, faults, and structural features are represented. Larger-scale maps (e.g., 1:10000–1:50000) capture finer geological variations and small-scale discontinuities critical for slope stability assessment, whereas smaller-scale maps (e.g., 1:200000–1:250000) tend to generalize such details, potentially reducing spatial precision. Several studies have demonstrated that higher-resolution inputs improve model accuracy [13], yet few have systematically compared the predictive performance of AI models across multiple geological map scales.

This study addresses this research gap by assessing the impact of geological map scale on the performance of four AI models: ANN, CNN, DNN, and CNN–DNN for landslide susceptibility zonation along the newly constructed Tuyen Quang–Ha Giang Highway in northern Vietnam. The analysis integrates 139 landslide locations with 14 conditioning factors encompassing topographic, geological, hydrological, and anthropogenic variables. Model performance is evaluated using the Area Under the ROC Curve (AUC) and several statistical indicators, supported by the SHAP (Shapley Additive Explanations) technique for interpretability. The results provide additional evidence on the influence of geological map scale on the performance and spatial representation of AI-based LSZ models, thereby supporting more informed selection of spatial data sources for landslide hazard assessment. Furthermore, the study highlights the robustness and interpretive power of deep learning, particularly the hybrid CNN–DNN model as an effective approach for developing accurate and scalable landslide susceptibility maps applicable to infrastructure planning and disaster mitigation in mountainous regions.

2. Study Area

This study focuses on the corridor of the Tuyen Quang–Ha Giang Highway, a 77.2 km long highway under construction in northern Vietnam. The alignment begins at Km0 (equivalent to Km9+268 of the Tuyen Quang–Phu Tho Highway) and terminates at Km77+200, within Tuyen Quang Province (Fig. 1). This region belongs to the midland and mountainous terrain of northern Vietnam, characterized by rugged topography, complex geological structures, and frequent mass movements. Elevations in the area range mostly between 200 and 600 m, interspersed with steep mountain ranges exceeding 1,000 m. The terrain is intensely dissected, forming steep slopes, narrow valleys, and deeply incised drainage networks. Such geomorphological features, combined with heavy rainfall and anthropogenic disturbances, make the area particularly susceptible to landslides.

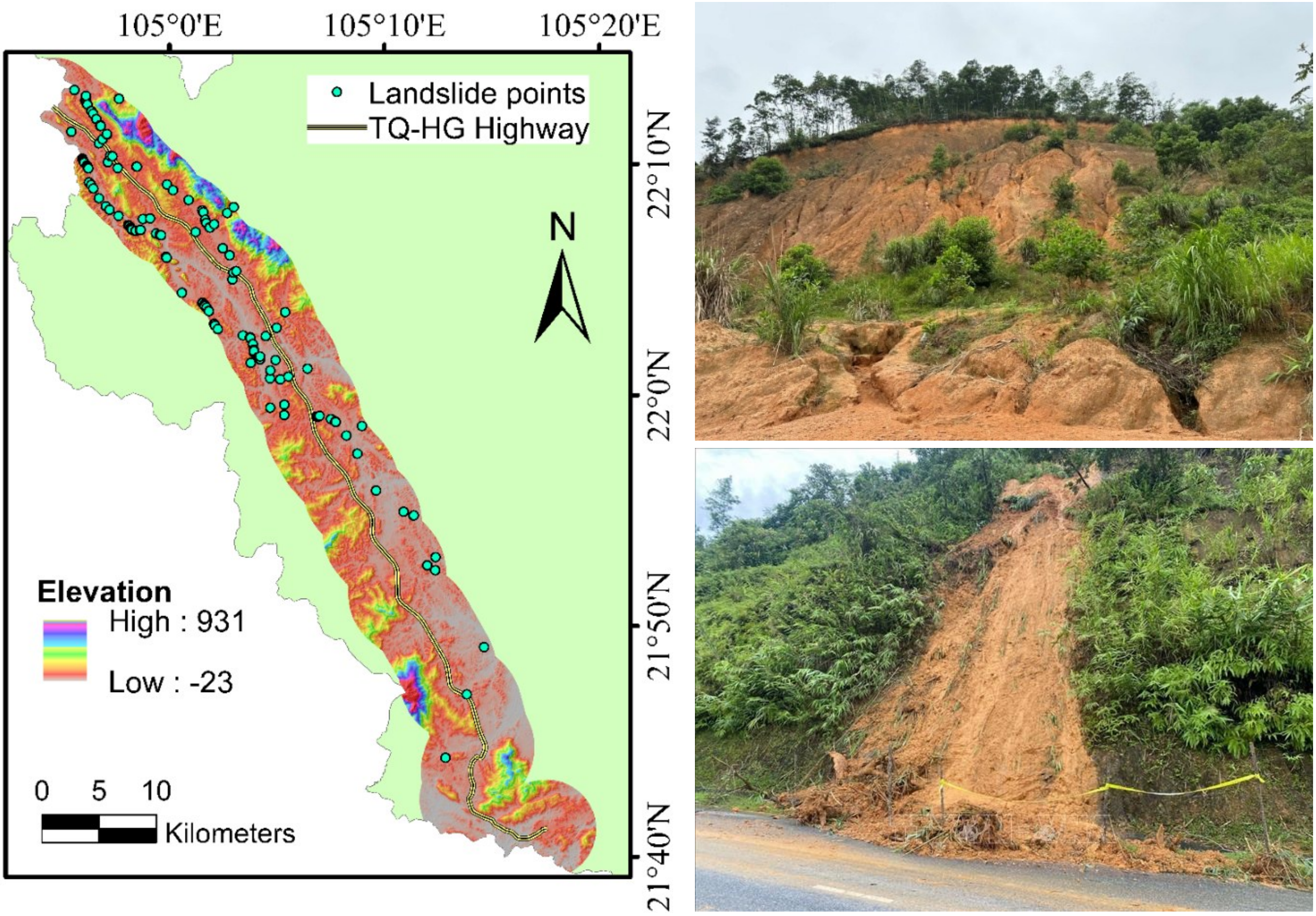

Fig. 1. Location map of the study area along the Tuyen Quang–Ha Giang Highway

2.1. Geological and structural setting

Geologically, the region exhibits a complex tectonic and lithological framework influenced by multiple fault systems, notably the Lo River, Tam Dao–Nghiem Son and Pho Day faults. The bedrock primarily consists of sedimentary and metamorphic formations interbedded with Quaternary deposits. Continuous tectonic deformation and prolonged weathering have produced a thick weathered crust with weak mechanical strength, high porosity, and elevated water saturation, resulting in reduced slope stability. The fault zones act as zones of weakness, facilitating groundwater infiltration and triggering slope failures, particularly during high-intensity rainfall events.

2.2. Climatic and environmental characteristics

The area lies within a tropical monsoon climate, receiving an average annual rainfall of 1600–2000 mm, with nearly 70% occurring between May and October. Frequent high-intensity storms, especially during the rainy season, contribute to toe erosion, rapid surface runoff, and slope saturation conditions that frequently initiate shallow and deep-seated landslides. Mean annual temperatures range from 22°C to 24°C, supporting dense but often disturbed vegetation.

2.3. Engineering geological conditions

The weathering mantle above bedrock varies in thickness from 2 m on steep slopes to more than 10 m in low-lying valleys. The upper layers are composed mainly of clayey to silty soils, often mixed with gravels, exhibiting low shear strength and high plasticity. On steep slopes, erosion and washout processes dominate, creating colluvial and residual deposits of low mechanical stability that are prone to slope failures, particularly along road cuts and construction sites.

3. Data collection and analysis

3.1. Landslide inventory

An accurate and comprehensive landslide inventory forms the foundation for reliable landslide susceptibility modeling. In this study, landslide data were compiled from three primary sources: (1) previously published reports, (2) interpretation of high-resolution Google Earth imagery and (3) detailed field surveys conducted using a GARMIN 64S GPS unit. The survey area extended approximately 4 km on either side of the highway centerline, covering the section from Km0+000 to Km77+200.

Table 1. Statistics of landslide points classified by magnitude, movement type, and slope origin

Landslide magnitude			Types of movement					Slope type	
Magnitude class	Landslide volume (m^3)	Number of landslides	Rotational slide	Translational slide	Complex movements	Debris flow	Rock fall	Natural slope	Cut slopes
Small	< 200	105	49	-	56	-	-	8	97
Medium	200-1000	31	11	-	20	-	-	4	27
Large	1000-20000	3	-	-	3	-	-	-	3
Very large	20000-100000	-	-	-	-	-	-	-	-
Extremely large	>100000	-	-	-	-	-	-	-	-
Total		139	60	-	79	-	-	12	127

Two systematic field campaigns were carried out to validate mapped landslides and record their characteristics. For each identified site, key parameters such as geographical coordinates, movement type, sliding material, slope geometry, and failure depth were documented. Integration of remote sensing and field data yielded 139 verified landslide points, which served as the core dataset for training and validating the AI models.

Spatial analysis presented in Table 1 shows that most landslides occurred in Ham Yen district (96%), where steep slopes, dissected topography, and road-cut excavations dominate. The majority were small-scale failures (<200 m³), accounting for 75% of all recorded events, while medium-scale (200–1000 m³) and large-scale (>1000 m³) landslides represented 22% and 2%, respectively. Notably, about 91% of landslides occurred on artificial slopes, emphasizing the influence of construction-related disturbances. Two primary failure types were identified: rotational slides (43%) and complex failures (57%), the latter often associated with deeply weathered bedrock and prolonged rainfall infiltration [14].

3.2. Landslide conditioning factors

The predictive success of LSZ models depends strongly on the appropriate selection of conditioning factors. Based on field evidence and prior research, 14 conditioning factors influencing slope stability were selected, encompassing topographic, hydrological, geological, and anthropogenic domains. These include elevation, slope, curvature, aspect, NDVI, Topographic Wetness Index (TWI), Stream Power Index (SPI), flow accumulation, average annual rainfall, maximum rainfall, geology, distance to faults, distance to roads, and distance to rivers (Table 2).

To evaluate the impact of geological map scale, the geological and distance to faults layers were prepared at two scales 1:50000 and 1:200000. All spatial datasets were standardized to a 12.5 × 12.5 m raster resolution to ensure consistency in analysis. The spatial distribution of the conditioning factors is illustrated in Fig. 2.

Table 2. Landslide conditioning factors used in the study

Factor	Scale	Source
Elevation (m)	12.5 m	USGS DEM
Slope (degree)	12.5 m	DEM
Curvature	12.5 m	DEM
Aspect	12.5 m	DEM
NDVI	12.5 m	Sentinel-2
TWI	12.5 m	DEM
SPI	12.5 m	DEM
Flow accumulation	12.5 m	DEM
Average annual rainfall	12.5 m	Vietnam Meteorological and Hydrological administration
Maximum rainfall	12.5 m	Vietnam Meteorological and Hydrological administration
Geological	1:200000; 1:50000	General Department of Geology and Minerals of Vietnam
Distance to faults	1:200000; 1:50000	General Department of Geology and Minerals of Vietnam
Distance to roads	Vector-derived; rasterized at 12.5 m	Natural Resources Environment
Distance to rivers	Vector-derived; rasterized at 12.5 m	Natural Resources Environment

Continuous variables (e.g., slope, elevation, rainfall, TWI, SPI) were reclassified using the Natural Breaks (Jenks) method, while categorical variables (e.g., lithology, distance classes) retained their native classifications. The Frequency Ratio (FR) technique was initially applied to evaluate each factor's correlation with landslide occurrence, supporting feature interpretation prior to AI model training [15].

The relationships between conditioning factors and landslide occurrence derived from the Frequency Ratio (FR) analysis revealed several important patterns [14]. Slope angle showed a strong influence, with slopes between 27° and 35° exhibiting the highest susceptibility (FR = 4.99), which corresponds well with typical road-cut gradients in the study area. Aspect also played a significant role, as northeast-facing slopes showed higher instability (FR > 1.70), likely due to the dominant rainfall direction. In terms of terrain morphology, concave slopes (FR = 1.43) were more prone to failure because they tend to accumulate surface runoff and loose materials. Elevation analysis indicated that lower areas (<50

m) had higher landslide density (FR = 1.55), reflecting material accumulation and poor drainage conditions.

Vegetation cover was another important factor, with sparsely vegetated areas (NDVI = 0.11–0.26) showing increased susceptibility (FR = 2.52). Rainfall conditions significantly controlled slope instability, as maximum rainfall exceeding 120 mm and annual rainfall greater than 2000 mm were associated with a substantial increase in landslide probability (FR > 2.3). Geological conditions also varied with map scale: at the 1:200000 scale, the Bong Son Formation exhibited the highest susceptibility (FR = 6.77), whereas at the 1:50000 scale, the Phu Ngu Formation showed the strongest association (FR = 4.17), reflecting improved lithological differentiation at the larger scale. Anthropogenic and structural factors were also influential, with landslides concentrated within 100 m of road corridors (FR = 6.04) and frequently occurring within 200–300 m of major fault zones (FR ≈ 1.9). These results highlight the combined effects of topographic, climatic, geological, and human-induced factors on landslide occurrence.

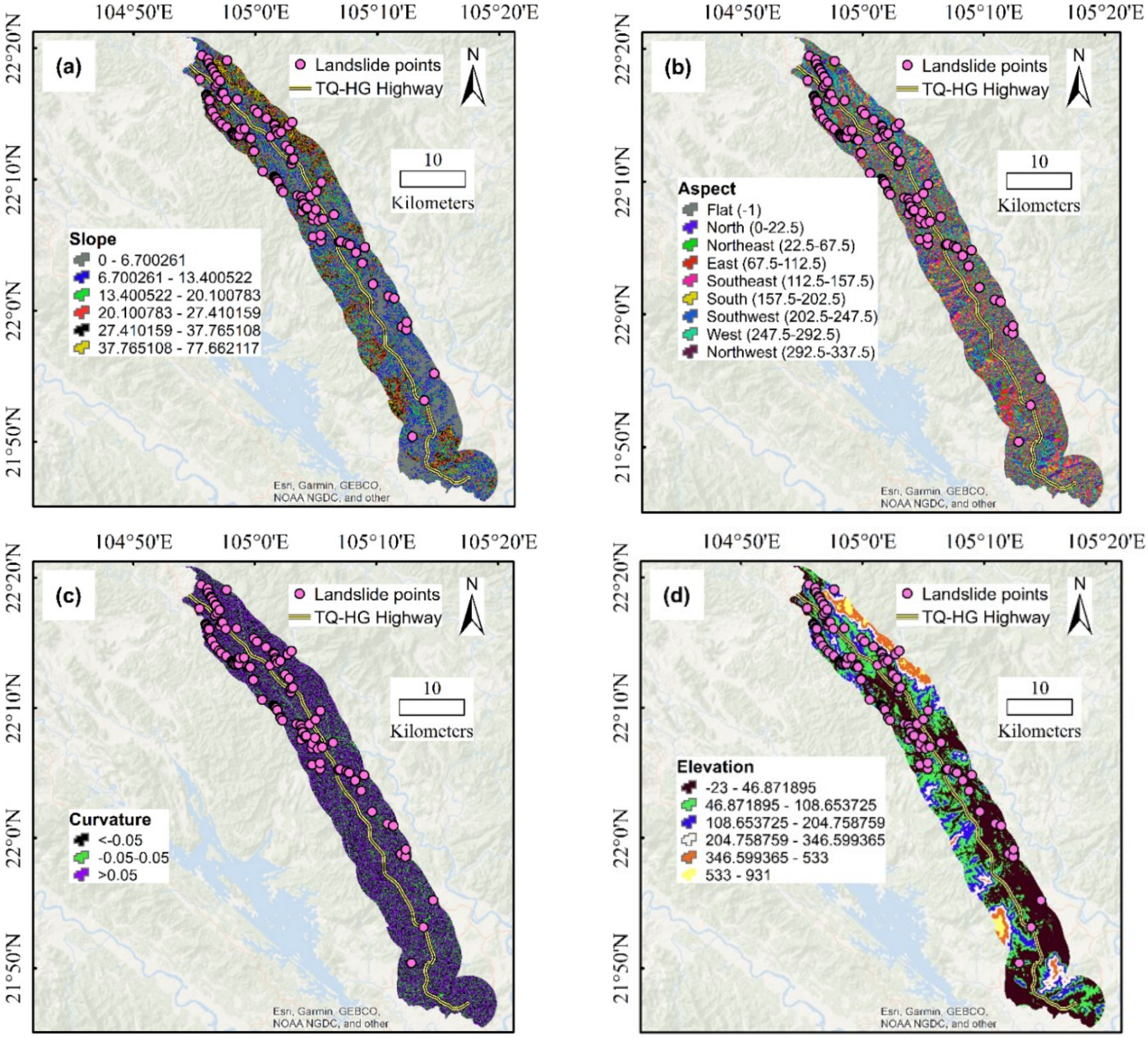

Fig. 2. Conditioning factor maps: (a) slope, (b) aspect, (c) curvature, (d) elevation, (e) NDVI, (f) TWI, (g) maximum rainfall, (h) annual rainfall, (i) flow accumulation, (j) SPI, (k) distance to faults (1:200000), (l) geology (1:200000), (m) distance to roads, (n) distance to rivers, (o) geology (1:50000), (p) distance to faults (1:50000) [14].

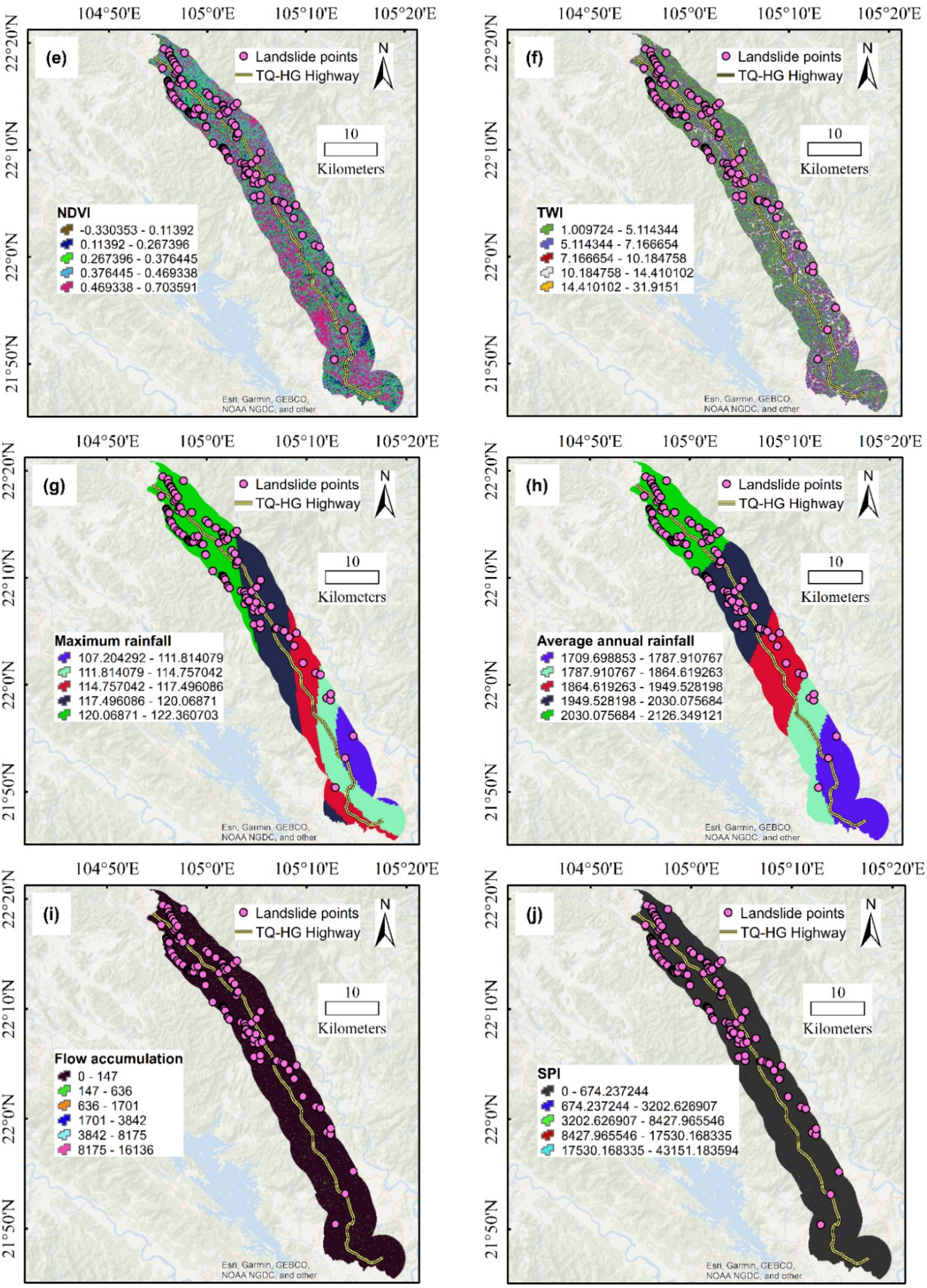

Fig. 2. (continued)

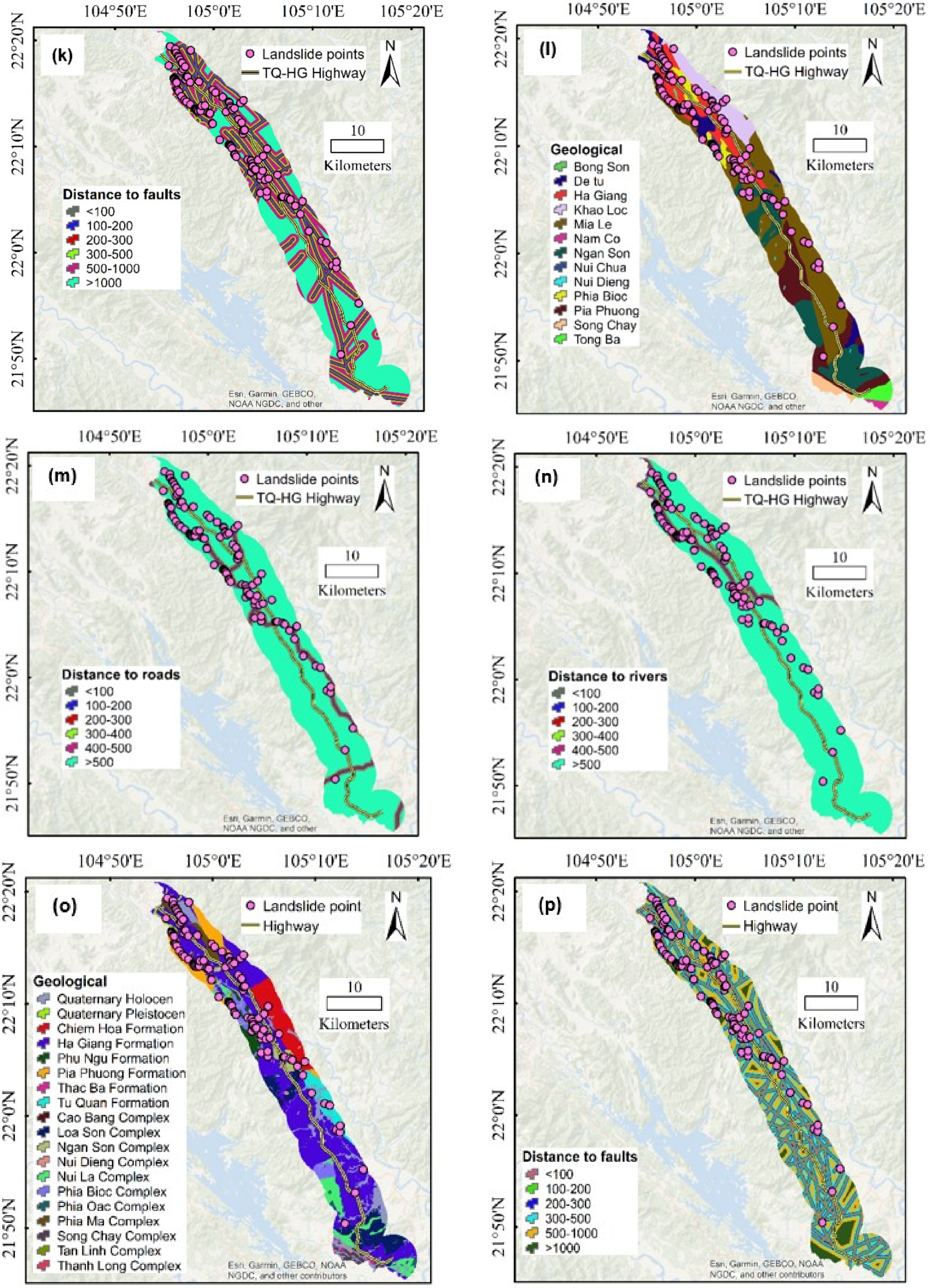

Fig. 2. (continued)

These analyses emphasize that rainfall, vegetation cover, slope geometry, lithology, and human activities are major controls on slope instability in the region. The differences in lithological detail between the two geological map scales are expected to influence model interpretation, motivating the comparative AI-based assessment in this study.

4. Methodology

The study employed four neural-network-based AI architectures, namely ANN, CNN, DNN, and a hybrid CNN–DNN model, to evaluate the impact of geological map scale on LSZ. ANN was used as a conventional feed-forward baseline model, while DNN represents a deeper fully connected architecture. Although CNN is also a type of ANN, it is specifically designed to extract local spatial patterns through convolutional operations. The hybrid CNN–DNN model was adopted to integrate CNN-based spatial feature extraction with DNN-based nonlinear prediction. These models were therefore selected as a progressive set of neural-network architectures capable of modeling complex nonlinear relationships between conditioning factors and landslide occurrence.

Model development and testing were conducted using Python 3.8 for AI implementation and ArcGIS 10.8 for geospatial data processing.

4.1. Artificial Intelligence models

4.1.1. Artificial Neural Network (ANN)

The ANN is a computational model inspired by the human brain, consisting of interconnected processing nodes, or neurons, arranged in input, hidden, and output layers [16]. Each neuron receives input signals, multiplies them by trainable weights, adds a bias term, and applies a nonlinear activation function, such as ReLU, tanh, or sigmoid. Through this structure, ANN can approximate nonlinear relationships between landslide occurrence and conditioning factors, which is essential for landslide susceptibility modeling because slope instability is usually controlled by the combined effects of multiple environmental variables rather than by a single factor. During training, the model continuously updates its weights using backpropagation and optimization algorithms to minimize prediction error. Although ANN has proven effective for nonlinear classification, its fully connected structure does not explicitly account for local spatial dependencies among neighboring raster cells. This may limit its ability to represent spatially complex terrain and geological conditions in landslide-prone mountainous areas.

The basic neuron computation is expressed as:

$$y=f(\sum w_i x_i+b) \quad (1)$$

where x_i= input values, w_i= weights, b= bias, and f= activation function.

4.1.2 Convolutional Neural Network (CNN)

The CNN architecture is optimized for spatial data such as images or gridded raster layers [17]. It uses convolutional layers to extract spatial features through localized kernels, followed by pooling layers that reduce data dimensionality and computational cost. Compared with fully connected models, CNN can help retain local spatial relationships among neighboring cells, which is relevant for landslide susceptibility zonation because slope instability may be affected by the spatial arrangement of terrain, geological boundaries, drainage conditions, and anthropogenic disturbances. Therefore, CNN is considered suitable for LSZ applications, where terrain and geological variables often show a certain degree of spatial continuity. However, its performance may depend on the quality and spatial resolution of the input raster layers, especially when geological information is represented at different map scales.

A convolution operation at location (i, j) can be expressed as [18]:

$$y_{i,j}=f\left(\sum_{c}\sum_{m}\sum_{n}\left(x^{(c)}_{i+m,J+n} * w^{(c)}_{m,n}+b\right)\right) \quad (2)$$

where $x^{(c)}$ denotes the input feature map of channel c, $w^{(c)}$ represents the convolution kernel weights, b is the bias term, and f(·) is the activation function.

4.1.3. Deep Neural Network (DNN)

The DNN extends the traditional ANN by incorporating multiple hidden layers, allowing the model to learn hierarchical data representations [11]. Each layer transforms input features into progressively more abstract representations, which may help capture nonlinear relationships among conditioning factors. This structure is relevant for landslide susceptibility modeling because landslide occurrence is commonly associated with the combined effects of multiple correlated variables, such as rainfall, slope, elevation, lithology, vegetation cover, and human-induced disturbances. Compared with a shallow ANN, DNN provides greater flexibility in representing complex factor interactions.

A DNN layer can be represented as:

$$a^{(l)}=f(W^{(l)}a^{(l-1)}+b^{(l)}) \quad (3)$$

where $a^{(l-1)}$= previous layer output, $W^{(l)}$= weight matrix, $b^{(l)}$= bias vector, and f= nonlinear activation function.

4.1.4. Hybrid CNN–DNN model

The CNN–DNN hybrid architecture integrates the spatial feature extraction strength of CNN with the hierarchical learning capacity of DNN, forming a robust model capable of both local and global pattern recognition [19].

In this framework, the input raster data are first processed through convolutional and pooling layers to extract spatial features from the conditioning factor maps. The extracted feature maps are then flattened and fed into multiple fully connected layers of the DNN to learn complex nonlinear relationships among features and to classify landslide susceptibility levels. The model is trained using backpropagation with the Adam optimizer and a cross-entropy loss function until convergence. This integration enhances prediction stability and accuracy, making the CNN–DNN model particularly effective for multifactor landslide susceptibility zonation problems characterized by heterogeneous spatial data and complex terrain conditions.

4.2. Validation metrics

The predictive performance of the models was primarily evaluated using the Area Under the Receiver Operating Characteristic Curve (AUC), which measures the overall ability of a model to discriminate between landslide and non-landslide areas across different classification thresholds [20]. The AUC is widely regarded as one of the most reliable indicators in landslide susceptibility studies because it is threshold-independent and reflects the generalization capability of the model. An AUC value greater than 0.9 indicates excellent predictive performance, while values between 0.8 and 0.9 represent very good model accuracy [21].

In addition to AUC, several complementary statistical indices were calculated to provide a comprehensive assessment of model reliability and classification performance. These include Positive Predictive Value (PPV), Negative Predictive Value (NPV), Sensitivity (SST), Specificity (SPF), overall Accuracy (ACC), and the Kappa coefficient (K), which measures the agreement between predicted and observed results beyond random chance. To further evaluate prediction errors and model stability, Root Mean Square Error (RMSE) and Mean Absolute Error (MAE) were also computed. The comparative analysis aimed to identify the optimal model characterized by high ACC, AUC, and Kappa values together with low RMSE and MAE, indicating superior accuracy and robustness.

4.3. Model Explainability – SHAP analysis

To enhance model interpretability, Shapley Additive Explanations (SHAP) were applied to quantify the contribution of each conditioning factor to landslide susceptibility predictions [22]. Beyond providing a ranking of variable importance, SHAP allows the direction and magnitude of each factor's influence on the model output to be examined. Positive SHAP values indicate an increased contribution to landslide susceptibility, whereas negative values indicate a reduced contribution. This is particularly relevant for landslide susceptibility zonation, where predictive performance should be supported by physically meaningful relationships between landslide occurrence and conditioning factors such as rainfall, slope, lithology, vegetation cover, elevation, and proximity to roads or faults.

4.4. Workflow and data processing

The methodological framework comprised six sequential steps to ensure scientific rigor and reproducibility:

- Data compilation: A total of 139 landslide points and 14 conditioning factors were standardized to a 12.5 m grid resolution.

- Preprocessing: All data were analyzed for correlation and normalized using the Min–Max scaler to the range [0, 1]. The correlation analysis in Fig. 3 shows that most conditioning factors exhibited weak correlations. The strongest correlation was observed between average annual rainfall and maximum rainfall (r = 0.94). This relationship is associated with rainfall-related triggering factors that cause landslide occurrence. Average annual rainfall reflects long-term moisture conditions that may contribute to slope weakening, whereas maximum rainfall represents short-duration extreme rainfall events that may directly trigger slope failure.

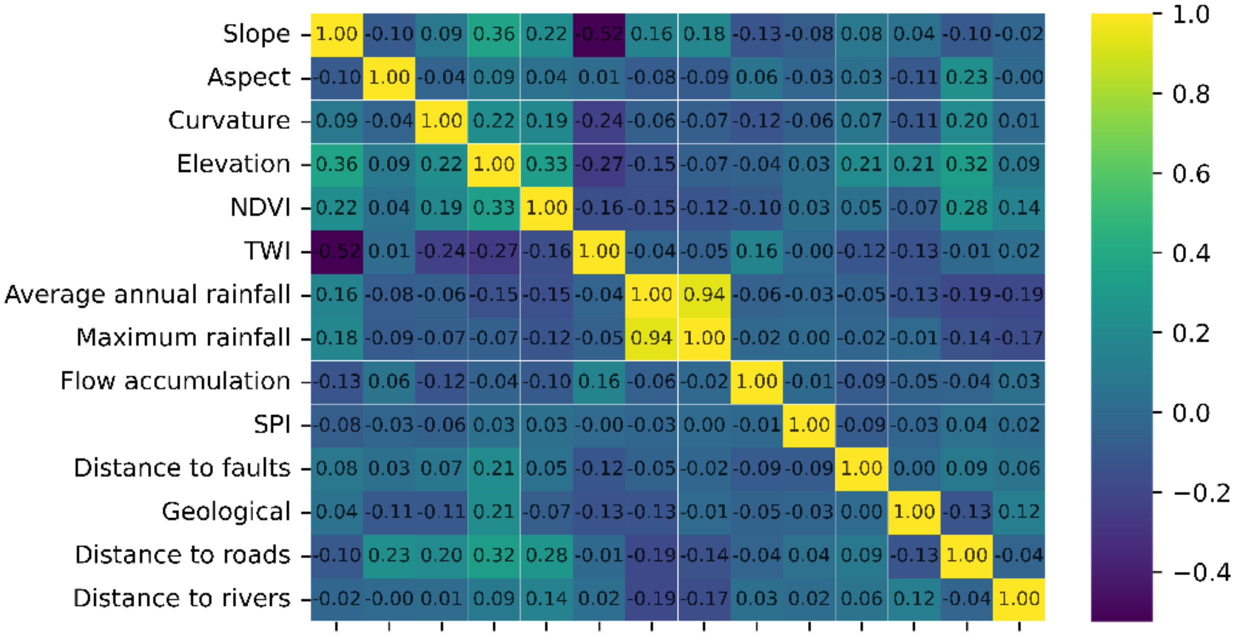

Fig. 3. Correlation analysis of the conditioning factors

- Dataset partitioning: Data were randomly divided into 70% training and 30% validation sets.

- Model training: Each AI model was trained using 10-fold cross-validation and optimized hyperparameters via grid search.

- Prediction and mapping: The output probabilities were reclassified into five susceptibility zones (very low to very high) using the Natural Breaks method in ArcGIS 10.8.

- Validation: Model outputs were compared with independent landslide points using FR analysis and landslide percentage distribution.

This systematic framework ensures both predictive accuracy and spatial reliability in LSZ outputs, as illustrated in Fig. 4.

5. Results and discussion

5.1. Model performance

The dataset was divided into 70% for training and 30% for validation to assess the predictive capabilities of the four AI models (ANN, CNN, DNN and CNN–DNN) at two geological map scales 1:200000 and 1:50000. All models achieved high AUC values (0.89–0.97), indicating strong predictive performance (Fig. 5). At the 1:200000 scale, the CNN–DNN hybrid model achieved the highest performance (AUC = 0.97), followed by ANN (0.92), while DNN and CNN recorded 0.91 each. At the 1:50000 scale, differences among models narrowed, but CNN–DNN remained superior (AUC = 0.97), suggesting that the hybrid architecture provided more stable predictive performance.

During validation, AUC values slightly decreased (0.88–0.93), with CNN–DNN maintaining the best stability (AUC = 0.93 at 1:200000; 0.92 at 1:50000). The hybrid model also achieved the highest accuracy (ACC > 88%) and Kappa coefficient (>0.74), alongside the lowest RMSE and MAE, underscoring its robustness (Table 3).

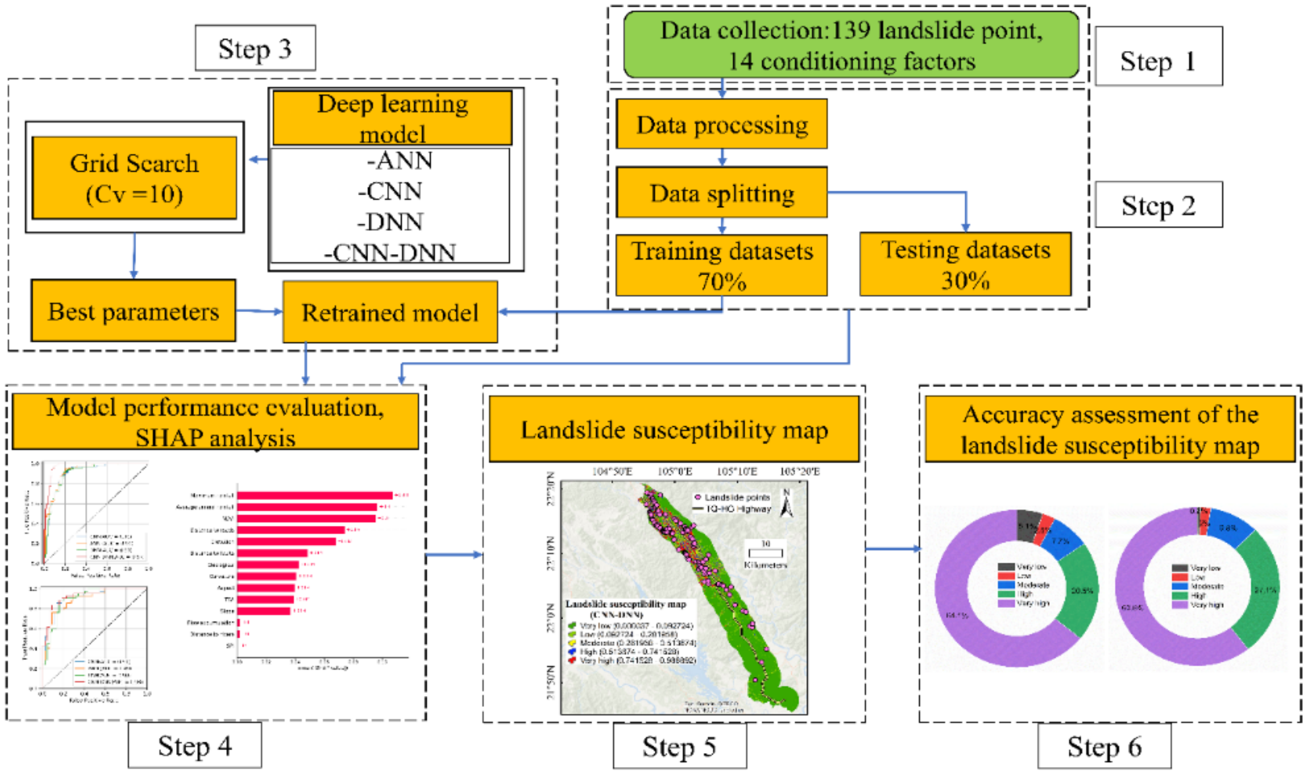

Fig. 4. Flowchart of the methodology used in this study

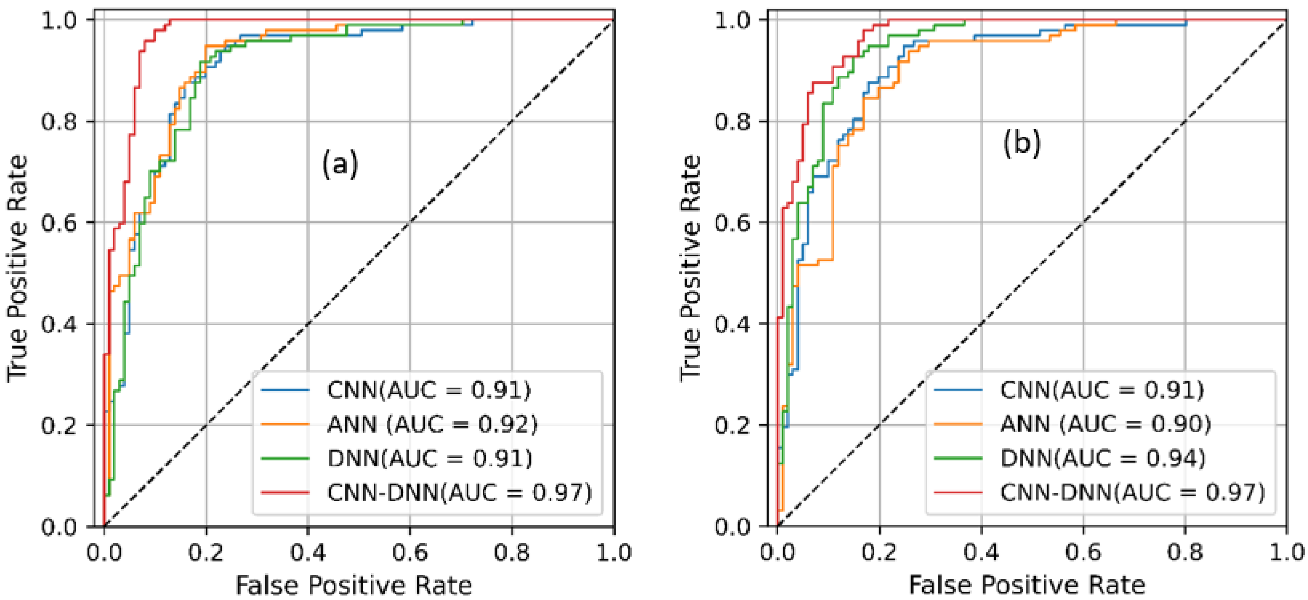

Fig. 5. AUC values of the models: training at (a) 1:200000 and (b) 1:50000; validation at (c) 1:200000 and (d) 1:50000

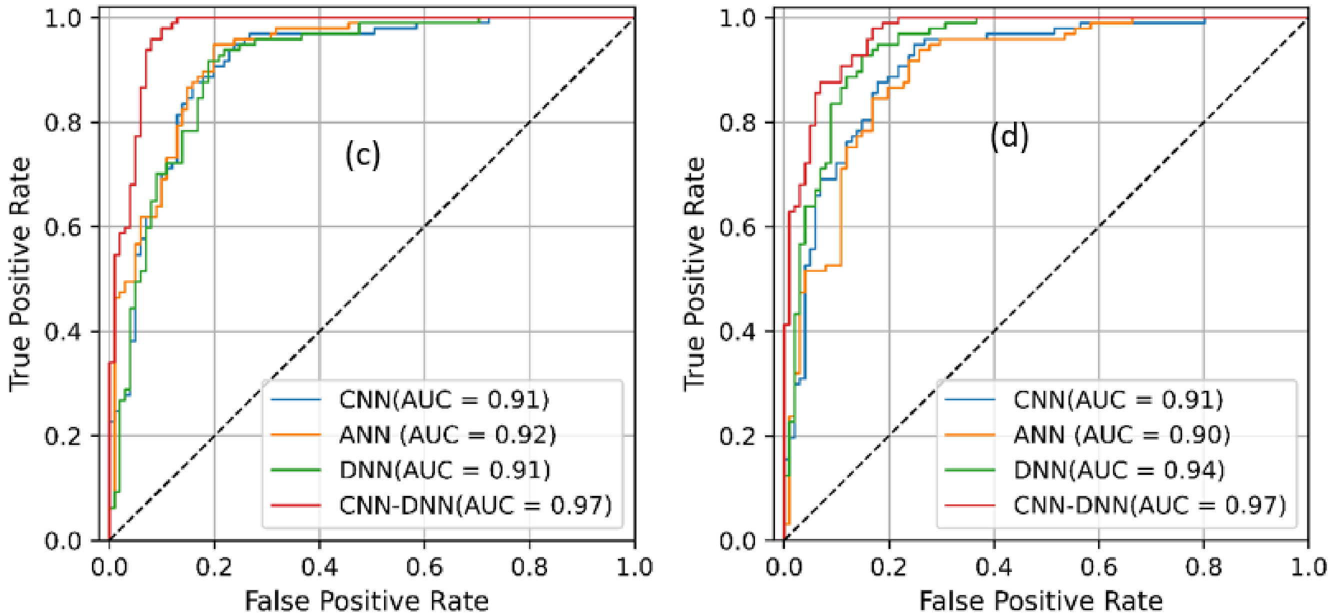

Fig. 5. (continued)

Table 3. Summary of model performance results at different map scales

No	Metric	Training performance				Validation performance			
		CNN	ANN	DNN	CNN-DNN	CNN	ANN	DNN	CNN-DNN
Map scale 1:200000									
1	TP	83	85	84	93	35	35	37	40
2	TN	86	87	86	88	37	37	38	36
3	FP	18	16	17	8	9	9	7	4
4	FN	11	10	11	9	5	5	4	6
5	PPV (%)	82.18	84.16	83.17	92.08	79.55	79.55	84.09	90.91
6	NPV (%)	88.66	89.69	88.66	90.72	88.10	88.10	90.48	85.71
7	SST (%)	88.30	89.47	88.42	91.18	87.50	87.50	90.24	86.96
8	SPF (%)	82.69	84.47	83.50	91.67	80.43	80.43	84.44	90.00
9	ACC (%)	85.35	86.87	85.86	91.41	83.72	83.72	87.21	88.37
10	K	0.707	0.738	0.717	0.828	0.675	0.675	0.744	0.767
11	MAE	0.146	0.131	0.141	0.086	0.163	0.163	0.128	0.116
12	RMSE	0.383	0.362	0.376	0.293	0.403	0.403	0.358	0.341
Map scale 1:50000									
1	TP	87	81	92	93	37	32	37	39
2	TN	79	84	83	84	33	36	32	36
3	FP	22	17	18	17	11	8	12	8
4	FN	10	16	5	4	5	10	5	3
5	PPV (%)	79.82	82.65	83.64	84.55	77.08	80	75.51	82.98
6	NPV (%)	88.76	84	94.32	95.45	86.84	78.26	86.49	92.31
7	SST (%)	89.69	83.51	94.85	95.88	88.1	76.19	88.1	92.86
8	SPF (%)	78.22	83.17	82.18	83.17	75	81.82	72.73	81.82
9	ACC (%)	83.84	83.33	88.38	89.39	81.4	79.07	80.23	87.21
10	K	0.677	0.667	0.768	0.788	0.629	0.581	0.606	0.745
11	MAE	0.162	0.167	0.116	0.106	0.186	0.209	0.198	0.128
12	RMSE	0.402	0.408	0.341	0.326	0.431	0.457	0.445	0.358

These results demonstrate that deep learning models, particularly the CNN–DNN hybrid, outperform conventional neural networks due to their hierarchical feature extraction and nonlinear learning capacity. The model's robustness across scales indicates that AI-based LSZ approaches can maintain predictive reliability even when input data resolution varies.

The SHAP analysis provided valuable insight into the relative contribution of conditioning factors to landslide occurrence in the CNN–DNN model (Fig. 6). At the 1:200000 scale, maximum rainfall exhibited the highest influence (0.11), followed by average annual rainfall and NDVI (0.10), while distance to roads and elevation showed moderate contributions (0.07). At the 1:50000 scale, the relative importance of the factors showed minor variations, with average annual rainfall becoming the most influential (0.11), followed by maximum rainfall and NDVI (0.09). Elevation and distance to roads also remained significant, with SHAP values of approximately 0.09 and 0.08, respectively.

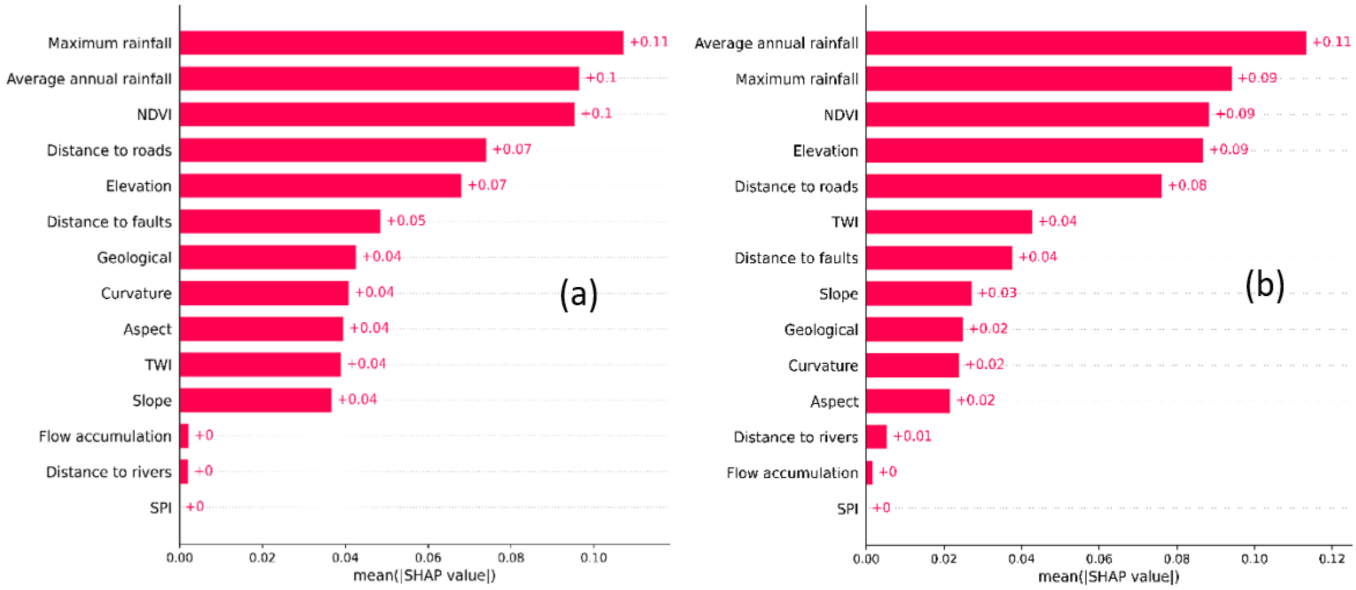

Fig. 6. SHAP value analysis of the CNN–DNN model at different map scales: (a) 1:200000 and (b) 1:50000

Overall, the results indicate that rainfall conditions, vegetation cover, elevation, and anthropogenic disturbances are the dominant controlling factors for landslide occurrence in the study area, whereas terrain-related parameters such as curvature, aspect, and SPI contributed comparatively less. The consistency of the key influencing factors across both geological map scales provides further evidence of the interpretability and stability of the deep learning model.

5.2. Landslide susceptibility mapping

Using the prediction results of the CNN–DNN model, landslide susceptibility maps were produced for both geological map scales. The model output probabilities were subsequently classified into five susceptibility levels: very low, low, moderate, high, and very high. This classification allows for a clear visualization of the spatial distribution of landslide susceptibility and provides useful information for hazard assessment, infrastructure planning, and risk management in the study area (Fig. 7).

The FR values generally increased from the very low to the very high susceptibility classes at both mapping scales, indicating clear differentiation among susceptibility levels (Fig. 8). The very high class at 1:200000 exhibited a higher FR value of 7.356 compared with 6.392 at 1:50000. However, validation showed that 64.1% of landslide points fell within the very high class at 1:200000, lower than the 69.1% observed at 1:50000 (Fig. 9). This difference indicates that FR reflects the relative concentration of landslides with respect to the area of each class, whereas the percentage of landslide points represents the proportion of validation locations within each class. Therefore, a higher FR does not necessarily correspond to a greater proportion of landslide locations.

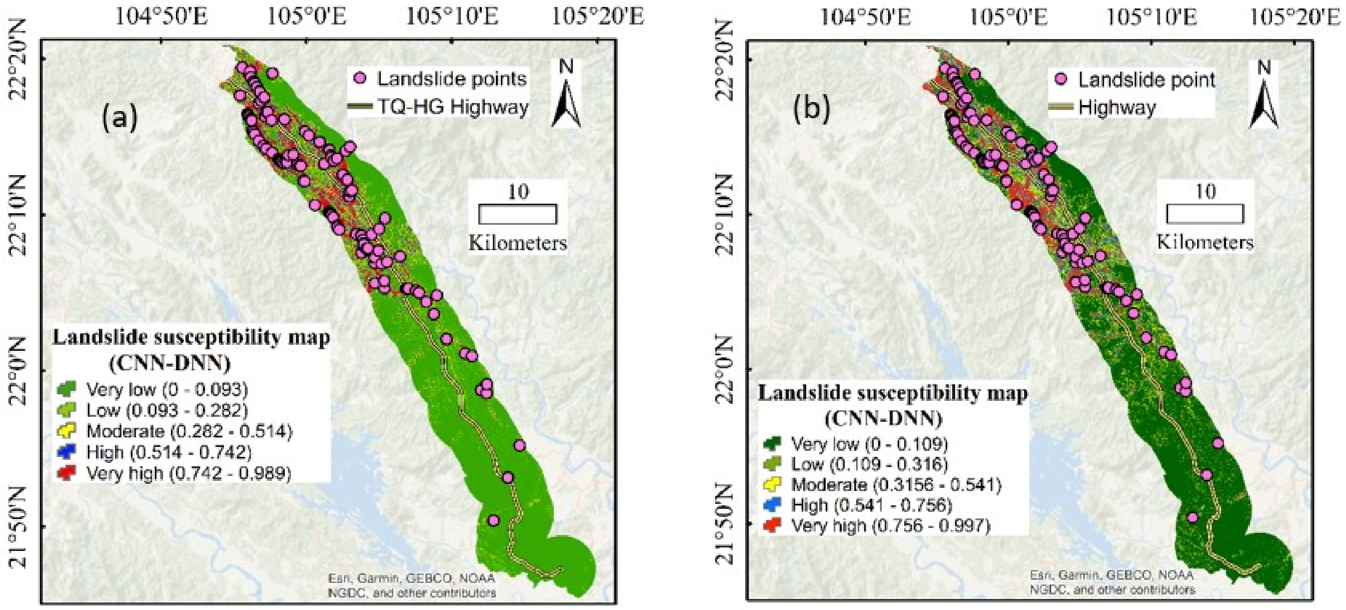

Fig. 7. Landslide susceptibility maps of the study area: (a) 1:200000 scale and (b) 1:50000 scale

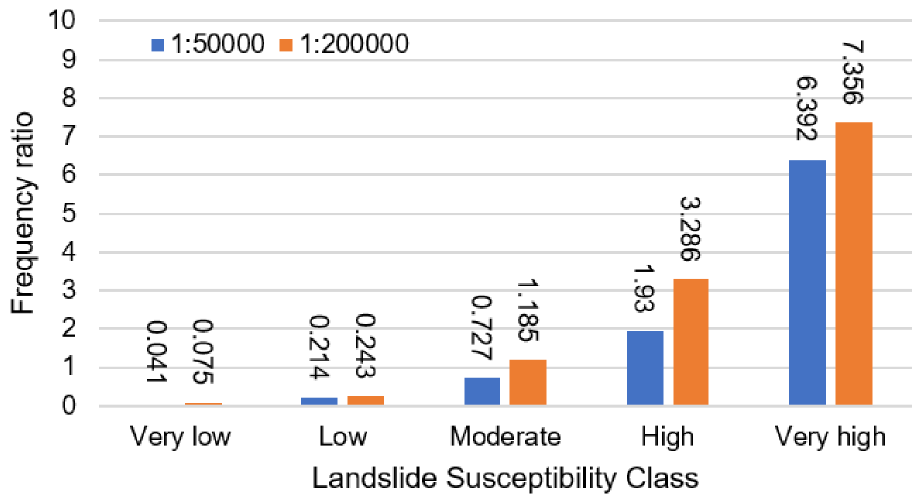

Fig. 8. Frequency ratio of landslide classes

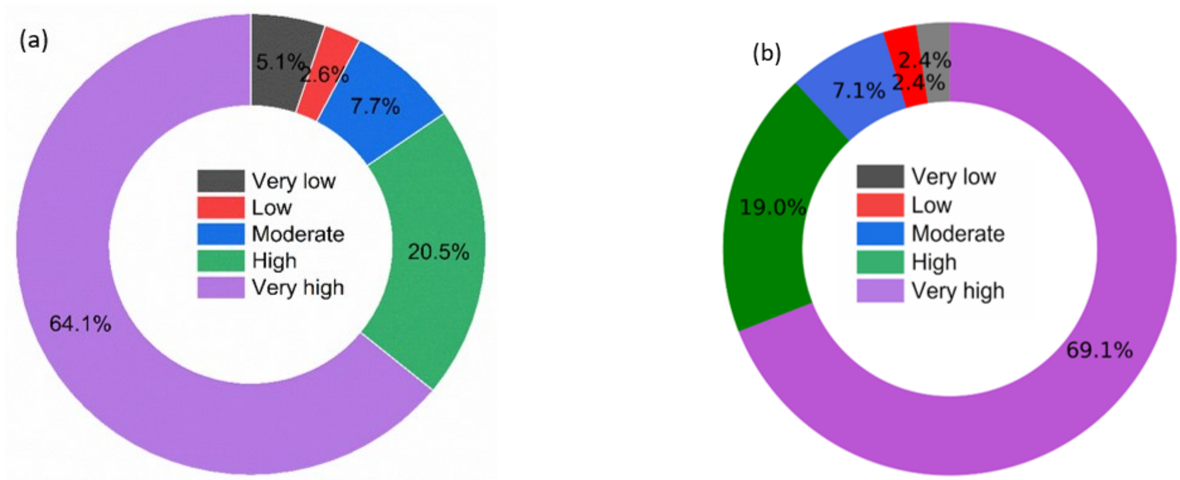

Fig. 9. Percentage of landslides by susceptibility class: (a) 1:200000 scale and (b) 1:50000 scale

These results demonstrate that map scale directly influences the spatial precision of LSZ outputs but not necessarily overall model accuracy. The enhanced resolution of the 1:50000 geological map allows finer discrimination of lithological and structural features critical to slope instability.

5.3. Comparative analysis and interpretation

The comparative analysis indicates that geological map scale affects AI-based landslide susceptibility zonation mainly through the spatial representation of susceptibility patterns rather than through large changes in statistical performance. Although both geological datasets supported relatively good model performance, their differences became more evident when the susceptibility maps were examined in terms of spatial detail, boundary definition, and local interpretability.

At the 1:50000 scale, the more detailed geological dataset allowed high-susceptibility zones to be delineated more clearly, especially in areas associated with steep terrain, fault-related structures, and lithological transitions. In contrast, the 1:200000 geological map provided a more generalized representation of geological units, which may smooth local variations and reduce the spatial precision of susceptibility zoning. This distinction is important because landslide susceptibility maps are not used only for statistical prediction, but also for identifying slope sections that require further investigation, monitoring, or mitigation.

The SHAP-based interpretation supports this spatial comparison by showing that the main controlling factors remained broadly consistent across the two geological map scales. Rainfall-related variables, vegetation cover, elevation, and road proximity were repeatedly identified as important contributors, suggesting that the model captured physically meaningful relationships between landslide occurrence and environmental conditions. Minor differences in factor importance between the two scales may reflect changes in how geological information interacts with other conditioning factors in the modeling process.

The comparison with recorded landslide locations further reinforces the practical relevance of geological map scale. The higher concentration of observed landslides within the very high susceptibility class on the 1:50000 scale map suggests better local agreement between predicted susceptibility and actual landslide occurrence. Nevertheless, the 1:200000-scale map still captured a substantial proportion of landslides in the high and very high susceptibility classes, indicating that generalized geological data remain useful for regional-scale hazard screening [23, 24].

Overall, the findings suggest that both geological map scales can support AI-based landslide susceptibility zonation, but they are suited to different levels of application. The 1:200000 geological map may be appropriate for preliminary or regional-scale assessment, whereas the 1:50000 geological map provides better support for detailed interpretation, highway corridor management, and prioritization of slope protection measures. Therefore, the selection of geological data scale should depend not only on model accuracy, but also on the intended use of the susceptibility map in practical hazard assessment and risk mitigation [25].

6. Concluding remarks

This study investigated the influence of geological map scale on AI-based landslide susceptibility zonation along the Tuyen Quang–Ha Giang Highway. The results show that the four AI models achieved good predictive performance at both geological map scales, namely 1:50000 and 1:200000. Among them, the CNN–DNN hybrid model showed the most consistent performance across the two datasets, suggesting that the integration of CNN-based spatial feature extraction and DNN-based nonlinear learning can improve the reliability of landslide susceptibility modeling. The assessment of susceptibility zoning results further showed that the 1:50000 geological dataset provided better outputs than the 1:200000 dataset, particularly in terms of spatial detail and the delineation of high- and very-high-susceptibility zones. This indicates that finer-scale geological information can enhance the spatial interpretation of landslide-prone areas, especially for infrastructure corridors in mountainous terrain. Although this study provides useful evidence on scale-dependent uncertainty, it was limited to two geological map scales. Future studies should incorporate additional map scales, higher-resolution topographic data, and multi-temporal rainfall information to further clarify how spatial data quality influences AI model performance and landslide susceptibility mapping outcomes.

Declaration of Generative AI

During the preparation of this work, the authors used ChatGPT (OpenAI) in order to improve the clarity of the manuscript and minimize grammatical and spelling errors. After using this tool, the authors reviewed and edited the content as needed and take full responsibility for the content of the published article.

References

[1]. M.J. Froude, D.N. Petley. (2018). Global fatal landslide occurrence from 2004 to 2016. *Natural Hazards and Earth System Sciences*, 18(8), 2161-2181. https://doi.org/10.5194/nhess-18-2161-2018

[2]. A. Addis. (2023). GIS-Based landslide susceptibility mapping using frequency ratio and Shannon Entropy Models in Dejen District, Northwestern Ethiopia. *Journal of Engineering*, 2023(1), 1062388. https://doi.org/10.1155/2023/1062388

[3]. A. Cemiloglu, L. Zhu, A.B. Mohammednour, M. Azarafza, Y.A. Nanehkaran. (2023). Landslide susceptibility assessment for Maragheh County, Iran, using the logistic regression algorithm. *Land*, 12(7), 1397. https://doi.org/10.3390/land12071397

[4]. B. Mandal, S. Mondal, S. Mandal. (2023). GIS-based landslide susceptibility zonation (LSZ) mapping of Darjeeling Himalaya, India using weights of evidence (WoE) model. *Arabian Journal of Geosciences*, 16, 421. https://doi.org/10.1007/s12517-023-11523-w

[5]. S.N. Selamat, N.A. Majid, M.R. Taha, A. Osman. (2022). Landslide susceptibility model using artificial neural network (ANN) approach in Langat river basin, Selangor, Malaysia. *Land*, 11(6), 833. https://doi.org/10.3390/land11060833

[6]. K. Prathom, C. Sujitapan. (2024). Performance of logistic regression and support vector machine conjunction with the GIS and RS in the landslide susceptibility assessment: Case study in Nakhon Si Thammarat, southern Thailand. *Journal of King Saud University-Science*, 36, 103306. https://doi.org/10.1016/j.jksus.2024.103306

[7]. M. Kanwar, B. Pokharel, S. Lim. (2025). A new random forest method for landslide susceptibility mapping using hyperparameter optimization and grid search techniques. *International Journal of Environmental Science and Technology*, 22, 10635-10650. https://doi.org/10.1007/s13762-024-06310-3

[8]. H. Nguyen, K.B. Dang, M.H. Nguyen, T.H. Nguyen, T.P.N. Pham, T.N. Do, M. Yasir, V.B. Dang. (2026). A multi-source framework for shallow landslide detection and warning in Da-river basin, Vietnam. *International Journal of Remote Sensing*, pp. 1-30. https://doi.org/10.1080/01431161.2026.2618102

[9]. B.T. Pham, V.D. Vu, R. Costache, T.V. Phong, T.Q. Ngo, T.-H. Tran, H.D. Nguyen, M. Amiri, M.T. Tan, P.T. Trinh, H.V. Le, I. Prakash. (2022). Landslide susceptibility mapping using state-of-the-art machine learning ensembles. *Geocarto International*, 37(18), 5175-5200. https://doi.org/10.1080/10106049.2021.1914746

[10]. S. Nikoobakht, M. Azarafza, H. Akgün, R.

Derakhshani. (2022). Landslide susceptibility assessment by using convolutional neural network. *Applied Sciences*, 12(12), 5992. https://doi.org/10.3390/app12125992

[11]. J.M. Habumugisha, N. Chen, M. Rahman, M.M. Islam, H. Ahmad, A. Elbeltagi, G. Sharma, S.N. Liza, A. Dewan. (2022). Landslide susceptibility mapping with deep learning algorithms. *Sustainability*, 14(3), 1734. https://doi.org/10.3390/su14031734

[12]. P. Varangaonkar, S.V. Rode. (2023). Lightweight deep learning model for automatic landslide prediction and localization. *Multimedia Tools and Applications*, 82, 33245-33266. https://doi.org/10.1007/s11042-023-15049-x

[13]. K. Katerina, S. Natalia, A. Emmanuel, K. Panagiota, I. Vassilis, P. Fotini, K. Garyfalia, P. Panagiotis, N. Nikolaos. (2026). Landslide Susceptibility Assessment in Greece: work in regional and national scale. *Natural Hazards*, 122, 437. https://doi.org/10.1007/s11069-026-08166-x

[14]. D.D. Nguyen, M.D. Nguyen, T.V. Nguyen, C.T. Cao, T.V. Phong, D.M. Duc, T.X. Bien, I. Prakash, H.V. Le, B.T. Pham. (2025). Enhanced landslide spatial prediction using hybrid deep learning model and SHAP analysis: a case study of the Tuyen Quang-Ha Giang Expressway, Vietnam. *Journal of the Indian Society of Remote Sensing*, 53, 1647-1666. https://doi.org/10.1007/s12524-024-02055-1

[15]. N. Fuad, J. Meandad, A. Haque, R. Sultana, S.B. Anwar, S. Sultana. (2024). Landslide vulnerability analysis using frequency ratio (FR) model: a study on Bandarban district, Bangladesh. *arXiv, arXiv:2407.20239*. https://doi.org/10.48550/arXiv.2407.20239

[16]. S. Mandal, S. Mondal. (2019). Artificial neural network (ANN) model and landslide susceptibility. *Statistical Approaches for Landslide Susceptibility Assessment and Prediction*. *Springer, pp 123-133.* https://doi.org/10.1007/978-3-319-93897-4_5

[17]. M.I. Sameen, B. Pradhan, S. Lee. (2020). Application of convolutional neural networks featuring Bayesian optimization for landslide susceptibility assessment. *Catena*, 186, 104249. https://doi.org/10.1016/j.catena.2019.104249

[18]. I. Goodfellow, Y. Bengio, A. Courville. (2016). Convolutional networks. Deep Learning, 2016, pp. 330-372. *The MIT Press.*

[19]. M. Azarafza, M. Azarafza, H. Akgün, P.M. Atkinson, R. Derakhshani. (2021). Deep learning-based landslide susceptibility mapping. *Scientific Reports*, 11, 24112. https://doi.org/10.1038/s41598-021-03585-1

[20]. H.R. Pourghasemi, O. Rahmati. (2018). Prediction of the landslide susceptibility: which algorithm, which precision? *Catena*, 162, 177-192. https://doi.org/10.1016/j.catena.2017.11.022

[21]. J. Huang, C.X. Ling. (2005). Using AUC and accuracy in evaluating learning algorithms. *IEEE Transactions on Knowledge and Data Engineering*, 17(3), 299-310. doi: 10.1109/TKDE.2005.50

[22]. H. Al-Najjar, B. Kalantar, B. Pradhan, G. Beydoun, N. Ueda. (2025). Shapley additive explanations (SHAP) for landslide susceptibility models: shedding light on explainable AI. *ISPRS Annals of the Photogrammetry, Remote Sensing and Spatial Information Sciences*, X-G-2025, 81-85. https://doi.org/10.5194/isprs-annals-X-G-2025-81-2025

[23]. N. Mebirouk, M. Amrane, S. Messast. (2025). Optimizing landslide susceptibility mapping in Oued Guebli Watershed: a comparative study of deep learning, support vector machines, logistic regression with spatial validation and AUC-ROC analysis. *Iranian Journal of Science and Technology, Transactions of Civil Engineering*, 49, 5981-6003. https://doi.org/10.1007/s40996-025-

01802-9

[24]. C. Polykretis, A. Faka, C. Chalkias. (2018). Exploring the impact of analysis scale on landslide susceptibility modeling: empirical assessment in northern Peloponnese, Greece. *Geosciences*, 8(7), 261. https://doi.org/10.3390/geosciences8070261

[25]. M. Ado, K. Amitab, A.K. Maji, E. Jasińska, R. Gono, Z. Leonowicz, M. Jasiński. (2022). Landslide susceptibility mapping using machine learning: A literature survey. *Remote Sensing*, 14(13), 3029. https://doi.org/10.3390/rs14133029